

# Topology in Sound Synthesis and Digital Signal Processing - DAFx2022 Lecture Notes

Georg Essl — University of Wisconsin - Milwaukee

November 2022

## Introduction

These are lecture notes accompanying a two part tutorial presented at DAFx2022 in Vienna on the topic of topology in digital signal processing and sound synthesis.

The purpose of the tutorial and hence the notes is to acquaint the attendees and reader with basic notions of topology that has proven useful in Digital Signal Processing and Sound Synthesis.

Topology and specifically algebraic topology is not a topic that is standard to a typical engineering mathematics education. Hence even basic concepts of this topic area are unknown to many practitioners in DAFx. The tutorial seeks to provide a rapid introduction in the topic while also focusing on why a DAFx researcher might benefit from learning about topology and using it in their work.

## Part I: Understanding Topology

What is topology? A useful intuition is to think of topology as "rubber-band" geometry (Figure 1). Imagine idealized rubber that can be stretched arbitrarily. There are certain properties the rubber maintains under deformation, and there are some that it does not. In particular, the stretching changes distances, while a rubber band in a loop configuration does not change the loopiness by stretching. Many useful topological constructions can sensibly be visualized using this intuition, despite its lack of formality. At times, other physical metaphors can also be useful as we will see later.

Slightly more precisely, one can think of topology as being concerned with the following: (i) Modeling connectivity, (ii) global invariants in a geometric setting (iii) independence from metric choices (or flexible choice of metric).

Practitioners in Digital Audio are very familiar regarding (i). We constantly model connectivity when we design filter structures, networks, use visual programming languages, and the like. The connectivity part of these constructions is known as graph theory, which is a combinatorial low dimensional theory in topology. However, both (ii) and (iii) may not be familiar concepts though it is quite likely that a practitioner in DAFx has seen them but perhaps not interpreted them as a notion related to topology.

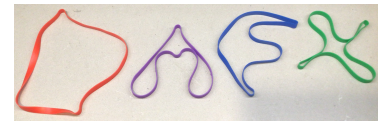


Figure 1: Rubber is a physical instance of material that is deformable, stretchable, while keeping its shape, such as that of a loop.

Ways of thinking about topology.

### Changing and Keeping Topology

For rubber we recognize that simply deforming and stretching a rubber band loop does not change that it is a loop. However, if we apply glue, or cut with scissors this changes things. A cut loop ends up being a string and can no longer hold jar lids in place. A glued rubber band may end up having more than one loop. Hence, adding connectivity and removing connectivity can change topology.

More strictly, however, this is a helpful intuition, but is not always correct. For example one can glue a rubber band in such a way that it ends up remaining a single loop. One can then conversely cut the glued band and again arrive back at the original loop. Hence if we think of topology as numbers of loops, we see that gluing and cutting may or may not change topology, and we have to be careful. However, in practice and with some experience, it remains a useful intuition because without gluing and cutting you are safe. Your rubber band does not change topology.

More formally, one wants to define when we have a topological equivalence. There are in fact numerous notions of topological equivalence that have different properties. A further approach is to categorize topologies computationally by some notion and define equivalences by those that have the same categorization. The second way of doing this is actually more practical and we will learn about it in Part II under the name *Homology*.

For an example of topological equivalence we will get a sense of the notion of *Homotopy*. Intuitively a homotopy is described by taking a piece of rubber string and moving it along a topological space. If you hit boundaries and are forced to wrap it around loops or other voids are formed, these constitute different homotopies. However moving along a surface otherwise is homotopic. This leads to the idea of a *deformation retract* which is shrinking all the space down that can be homotoped without obstruction. In other words "deformation retracts" capture changes in the space that do no change the *homotopy type*. For example if you have a disk you can shrink that to a point. Figure 2 shows the deformation retract from an annulus to a circle.

We will not look at homotopy computationally. Instead it is the generally assumed underlying equivalence that tells us if two topological configurations are the same or different. We will at times augment these equivalences with extra information, but the base equivalence will be homotopy throughout our discussions. Mathematicians like to say that we are working "up to homotopy".

Cutting and Gluing can change Topology.

Topological Equivalence.

Homotopy as sliding a rubber string over a topological space.

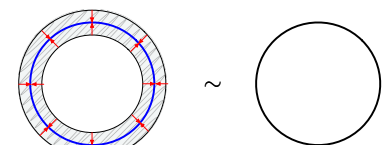


Figure 2: A deformation retract of an annulus to the circle.

We work "up to homotopy."

*Making Loops: Quotient Topologies*

Repetition are important in almost anything we do in Digital Audio and a loop is a characterization of repetition. Hence loops are important, and it is interesting to know how to make loops.

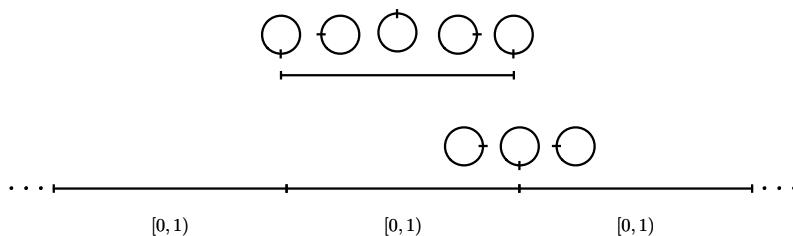
Taking a rubber band we can glue its ends together to form a loop. We can formalize this by "taking the quotient" or alternatively forming a "quotient topology".

By taking two entities and declaring them identical, one makes things previously separate into one. To illustrate this, we start with a piece of string and further assume that we can think of it as the line segment with the interval  $[0, 1] \in \mathbb{R}$ . This metric choice is for our mental convenience, as well as useful, as it relates to many practical settings, but it is not a restriction. If we chose an identification of the beginning of the line segment at 0 with its end at 1 we form an equivalence relation  $0 = 1$ . More generally, we can relate whole classes under equivalences, aptly called *equivalence classes*.

By having identified 0 and 1, they are no longer separate entities, hence our domain changed  $[0, 1)$  (as the 1 is now just the 0).

There are a few ways one can think of this construction as seen in Figure 3. If we do not insist on the flatness of the depiction of the domain, we see that it can be thought of as a parametrization of a circle. The identified flat line has an apparent jump while the circle is nicely continuous. It is also not obvious how one could apply a kind of rubber band analogy to describe the relationship.

One way out of this is by a relationship that we will call (un)rolling. Another way to form the same intuition is by (un)winding.



At the top of figure 4 we see the circle rolling along the line and a one-to-one correspondence between the line contact and the circumference position on the circle. Hence a repeated "unrolled" line actually captures the continuous nature of the circle in a flat fashion. The winding intuition comes from holding the circle fixed and winding an infinite rubber string around the circle and marking the positions where the winding repeats. If we then unwind again and lay down the string we arrive at the identical situation as depicted in figure 4. In the winding case it is more obvious that the wound string

Making loops by taking quotients.

$[0, 1]$  as a model of a flat line.

Equivalence classes are entities that are defined to be identical.

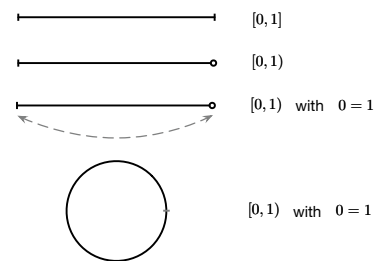
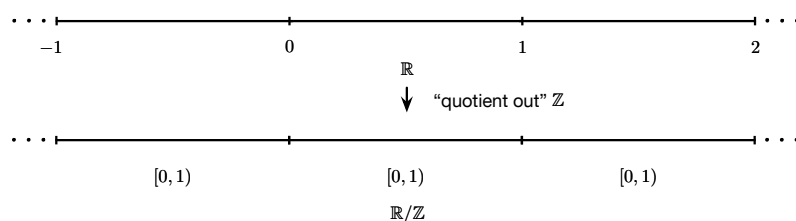


Figure 3: Forming a flat circle by identifying two ends of a line segment.

Figure 4: Rolling a circle on a line. The circle can roll over repeated segments of the line indicating that the circumference continues without obstruction.

covers the circle. If we just wind a finite amount of times we would call the result just a cover. If we create a winding that encapsulates all possible covers (we wind indefinitely as there is no obstruction to winding) we arrive at what is called the *universal cover*.

While we have been discussing flat lines and circles at this point it is important that this argument is — pun intended — substantially more flexible. Imagine a square with a circumference of 1 and we wind a rubber string around it as before and we mark repetitions. We arrive at the identical image as before. In fact we can do this for any path-like loop. Imagine that there are concave parts and we force the rubber into its nooks but then unwind to check the cover: we again arrive at the same cover. In short, these pictures are topological and are robust under deformation. We observe from Figure 5 that



Universal Cover of the circle is the infinite line with segmented repetition.

Figure 5: "Modding out"  $\mathbb{Z}$  from  $\mathbb{R}$  ( $\mathbb{R}/\mathbb{Z}$ ) creates an infinite segmentation of identical intervals  $[0, 1)$ .

the line segment repeats, but also that we can keep track of how many windings (or rolls) we have performed. So we can count the windings. This is a way to characterize a circle. Mathematicians call this count the *fundamental group* and a typical depiction of it can be seen in figure 6.

Notice that this is actually the same picture as the relationship of the circle and it rolling on an infinite line, except that we picture the line as a winding helix above the circle. This allows us to depict the counting as the points on the helix above a base point on the circle. The helix can be projected onto the circle (map  $P$ ) which also motivates the use of the symbol  $\pi_1$  for the fundamental group. The integers  $\mathbb{Z}$  under addition capture counting (and form a group, hence the name).

Again, this depiction does not depend on the precise shape of the circle but really applies to topological loops. We actually have good intuitions for this. We understand that for race tracks that are in a loop configuration, even if it is not a perfect circle, we can observe the number of laps a racer has performed.

By forming the quotient  $\mathbb{R}/\mathbb{Z}$  (say " $\mathbb{R}$  mod  $\mathbb{Z}$ ", or we "mod out  $\mathbb{Z}$ ") which means we identify all possible windings, we arrive at the same circle and again generate an interval domain of  $[0, 1)$ . For this reason, we consider the following interchangeable:  $[0, 1)$ ,  $\mathbb{R}/\mathbb{Z}$ , and  $S^1$ . This is computationally relevant, as it indicates that if we parametrize a loop

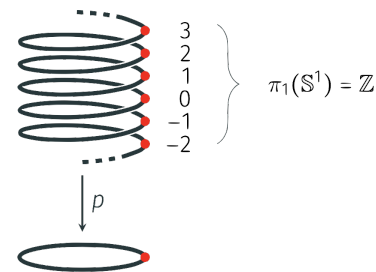


Figure 6: Fundamental group of the circle.

$[0, 1)$  is  $\mathbb{R}/\mathbb{Z}$  is  $S^1$ .



by  $[0, 1)$  computations on the loop follow arithmetic operations "mod 1". We will coin a circle that looks like the interval  $[0, 1) \in \mathbb{R}$  the *flat circle* given that its local metric looks like the flat line but suggesting that we are dealing with a circular topology.

The flat circle.

### Dynamics on Loops

One area of application of the above loop topologies is in dynamics. We want to evolve time over a space that repeats or is periodic. The canonical example is sinusoidal oscillation which can be thought of as the orthogonal projection of a dynamics on the circle.

Topological space as the domain on which dynamical evolution operates.

$$\sin(2\pi \cdot n \cdot t) = \Re \left( e^{i2\pi \cdot n \cdot t} \right)$$

Sine as orthogonal projection of the circle in the complex plane.

In the study of dynamical systems it is typical to consider evolution on some domain. This is implied in the above notation but not explicit. We can make it explicit in the following fashion. Our domain is a topological space equivalent to  $S^1$  parametrized by  $[0, 1)$ . This parametrization we can variably think of as a position on the circumference, or as the angle. A dynamical process is a map from one domain to another. In our case we want to describe the dynamics on a loop (for now a circle). Because we want to stay close to discrete computational methods we only consider discrete time dynamics. Further we will only consider time stepping that only depend on the previous time location. Hence we can describe a future position on the domain  $x_n$  as a function  $f$  of the previous position  $x_{n-1}$ , which we write as  $x_n = f(x_{n-1})$ . From our previous discussion we know that "mod 1" arithmetic will enforce the circle topology. We will call the discrete time functions *iterative phase functions* (see Figure 7). A discrete time series algorithm analogous to the sine oscillator above could hence be written as follows:

Iterative phase functions describe maps from the circle to itself in terms of discrete time steps.

$$\underbrace{y_n}_{\text{Time Series}} = \underbrace{p}_{\text{Projection}} \left( \underbrace{x_n = f(x_{n-1})}_{\text{Iterative Phase Function}} \underbrace{\text{mod } 1}_{\text{Circle Topology}} \right) \quad (1)$$

Given the discussion of the interchangeable description of flat circles we can define these functions in multiple equivalent ways:

$$f : S^1 \rightarrow S^1 \quad f : \mathbb{R}/\mathbb{Z} \rightarrow \mathbb{R}/\mathbb{Z} \quad f : [0, 1) \rightarrow [0, 1)$$

Circle maps are maps from the circle to itself.

Study of these maps are known as *circle maps*. Observe that in equation (1), we have abstracted what would be the orthogonal projection of a sine oscillator into an unspecified projection function.

This is because written this way we see that projection and computation of dynamics on the circle topology are actually independent of each other, hence we are freed up to pick other projections.

We can recover a discrete version of the sinusoidal oscillator the following way:

$$y_n = \sin(2\pi \cdot \phi_n) \quad \phi_n : x_n = x_{n-1} + \Omega \pmod 1$$

where  $\Omega$  is a constant. Hence we step around the circle with constant step sizes.

A large class of oscillatory techniques in sound synthesis can be formulated in this way <sup>1</sup>. Our goal here is to focus on the topological aspects and hence we will not have time to discuss them. An important topological generalization worth observing is that given that we have iterative phase function on the interval  $[0, 1)$ , these functions are in principle applicable to any homotopy of that interval! An application of this insight was presented at DAFX2022 during the paper session.

Another topological notion worth mentioning is that arithmetic "mod 1" is *topologically stable* in the following sense: Given that a circle is compact and that the arithmetic forces all computations onto the compactness of the circle, the computation can never grow out of bounds. This is not true for iterative maps that are not defined on a circle domain such as the logistic map, which can become unstable when parameters do not fall into a controlled range.

### Folded Circle

The orthogonal projection of the circle as computed by the sinusoid has a property that we can study topologically. Due to the orthogonal projection, we get two extrema of the circle. This gives us some extra structure that is not captured by homotopy.

We will capture this notion by marking the two extrema, but also by adding markings to the two paths connecting the extrema as depicted in Figure 8. As we roll this circle on the real line we observe that the two sides alternate. If we want to construct an analogy to the flat circle from before, we can simply flatten out the circle and we arrive at a two flat lines with sharp folds at each end (giving this construction its name). Here an analogy to folding and creasing paper is useful. We can further construct a version of a helix-like cover that keeps the fold points marked. This picture is again just a different way of depicting the real line with folding points marked. If we skip every other fold point, we arrive at the standard flat circle. In other words the folded circle is a flat circle with "extra structure".

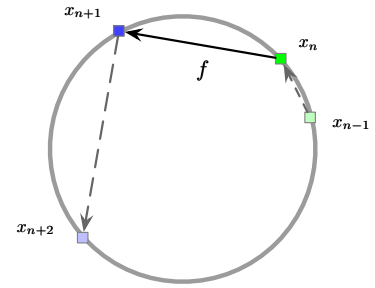


Figure 7: Iterative phase functions  $f$  describe discrete steps from a position on the circle to another.

<sup>1</sup> Georg Essl. Iterative phase functions on the circle and their projections: Connecting circle maps, waveshaping, and phase modulation. In Richard Kronland-Martinet, Sølvi Ystad, and Mitsuko Aramaki, editors, *Perception, Representations, Image, Sound, Music*, pages 681–698. Springer, 2021. ISBN 978-3-030-70210-6

Topological stability denotes the stability of a numerical algorithm due to the underlying topological domain. Maps from the circle to itself are topologically stable.

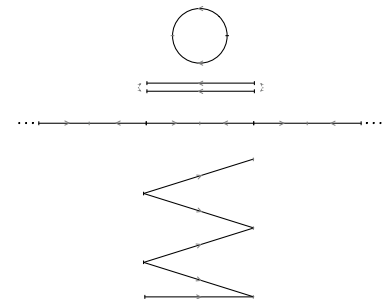


Figure 8: Different depictions of the Folded Circle.

### Aliasing and Sampling

Steiglitz's *Six Domains of Signal Processing*<sup>2</sup> shown in Figure 9 provide a very nice pictorial relationship of aliasing, sampling, and duality under Fourier-style transforms for various forms of signal processing. It depicts the relationship between infinite continuous time signals (also known as *analog* signals), the sampled discrete signal thereof, and short-term windowed signals (with a periodicity assumption). Via duality of the respective transforms we arrive at the respective frequency domain versions and one observes that sampling is dual to aliasing.

It is rather typical to think signal first, hence we think sampling first. However, for our purpose, aliasing is the more interesting phenomenon as we have a topological way to describe the phenomenon now. We observe that aliasing is the consequence of "modding out  $\mathbb{Z}$ " hence leading to the fundamental group  $\mathbb{Z}$  counting the multiplicity of reaching any point on the quotient topology. The map in Steiglitz's diagram labeled "aliasing" moves a non-quotiented entity onto a quotiented one and this means that one repeatedly wraps around the former around the latter (one can again use the winding or rolling metaphor here).

As is well known to practitioners in digital audio, sampling and aliasing are related. They are dual under a Fourier-style transform. This relationship can be seen nicely in the six domains. It turns out that this duality is a special case of a more general duality: the *Pontryagin duality*, which holds for locally compact topological groups.

Given that the aliasing picture in Figure 9 involves the complex circle and its real projection, we are dealing with the topology of a folded circle. It is well known in signal processing that frequencies just above the Nyquist (sometimes also call folding) frequency "folds over" as it passes that frequency. By the same token it also requires that negative frequencies "fold back" at the bottom of the spectrum in a similar fashion. Folding diagrams (Figure 10 shows an example) describe this property metrically, but topologically they look like the folded cover of Figure 8 (bottom). Hence we can understand the observed folding behavior to stem from the topology of the folded circle.

### Fourier Analysis of the Wave Equation as Aliasing and Sampling

Rather than sample first one can also chose to alias first. Much of what we just discussed pertains unchanged though it deserves a different physical interpretation. This process then again leads to six domains, which this time we call *Six Domains of the Wave Equation* as depicted in Figure 11.

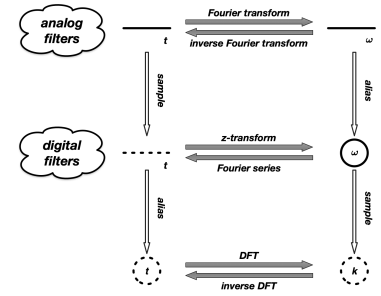


Figure 9: Six domains of Signal Processing.

<sup>2</sup> Ken Steiglitz. *A Digital Signal Processing Primer, with Applications to Digital Audio and Computer Music*. Addison Wesley, 1997

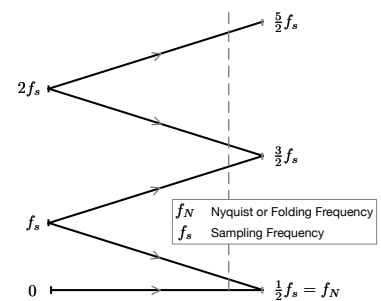


Figure 10: The folding diagram is a metric version of the cover of the folded circle.

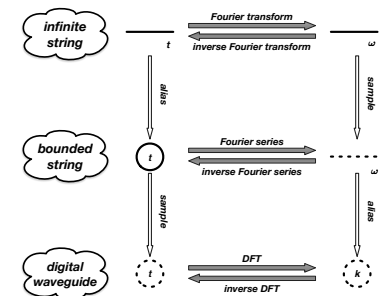


Figure 11: Six domains of the Wave Equation.

Introducing boundary conditions leads to a folded circle, for which the dual is samples. However, now the time and frequency domain is switched, and the resulting picture captures the well-known fact that the finite string has a discrete (though infinite) spectrum. By sampling the finite string, we arrive at a waveguide-style discretized model of the wave equation which has an aliased discrete spectrum. The unfolding of the bounded string is a well-known property in specific settings. Taking the traveling wave solution one can use the boundary condition to derive the reflection function, which turns out to have an equivalent image behind the boundary that travels towards the reflection point from behind as a wave to be reflected travels towards (see Figure 12). This pattern repeats for each length of the string. We should now recognize this as nothing but the "unrolled" string, i.e. its universal cover.

There is a third way to depict this situation (Figure 13). This move is similar with an unfold, though we merely "lift" the flat propagation directions into a circle. This change already has a noteworthy effect. If arrows move left and right on each branch, in the circle depictions their apparent motion is always forward, hence the unfolding has turned abrupt bounces into smooth motion.

### *Using Covers to Study Dynamics of Reflections*

Figure 13 illustrates the circle topology of the bounded string, but it is rather specific in its impulsive propagation. A way to think about topology is ways to capture behavior that no longer relies on specific details. Here we give a construction that generalizes traveling impulses and gives us a topological interpretation of the impact of boundary conditions. Rather than model the impulse propagation, we instead merely capture the state of an impulse over the range of the circle between boundaries. We observe that the up/down direction of the impulse does not actually change between boundaries and that this is true even under variation. If the impulses were damped or travelled irregularly they would still retain their up/down orientation between boundaries. So rather than model the impulse, we will simply create a lift of a path for each impulse color (green and blue) that captures its up/down state between the range. This construction yields the configuration depicted in Figure 14.

This is a topological picture that captures a range of changes in impulses, but it also allows us to clarify that of course we require that the travel-topology, i.e. the paths that the impulses can take do not change under an assumed variation. For example if there is a scatterer introduced, that would change the way impulses travel and the above construction does not contain this case. This depiction of

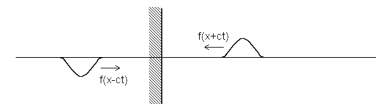


Figure 12: Reflection of a traveling wave at a boundary. A virtual image equivalently travels towards the reflection from behind the reflection point.

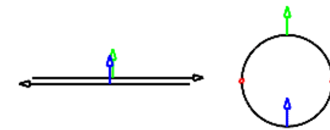


Figure 13: An impulse load on a waveguide in flat configuration as well as in a lift onto a circle.

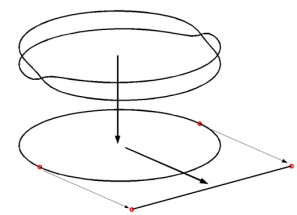


Figure 14: The up/down state of traveling impulses is captured as a lifted cover over the circle, yielding a double cover.

wave reflection is, despite its simplicity, still insightful, as can be seen in Figure 15. Moving around the circle once corresponds to moving

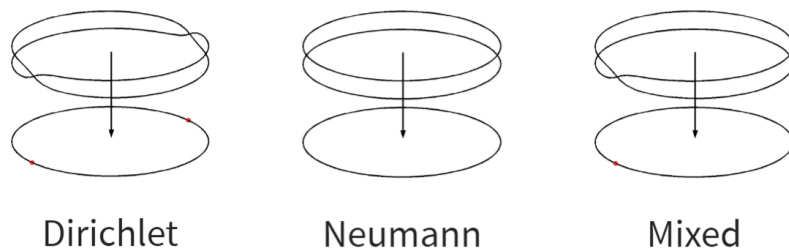


Figure 15: Double Covers for Dirichlet, Neumann, and Mixed boundary conditions. The last is equivalent to the cover of a Möbius strip.

along the bounded wave domain twice, and we observe that both Dirichlet and Neumann conditions share that property. However, the mixed boundary condition leads to a double cover that requires rotation about the circle twice to return to the starting point in the same state. This is the well-known behavior of the Möbius strip. This also leads to comparative behavior. Given that it takes twice as long to complete a "period", the mixed boundary should be half the fundamental pitch. This is of course well known for instruments such as clarinets or one-sided capped organ pipes compared to their open counterparts such as flutes and open-ended organ pipes. The elegance of this argument is that it is quite general. As long as we have no scattering we can expect this behavior, hence we have found a description that we expect to hold even if we do not have a precise solution to compute a specific case.

### *The Flat Torus*

The flat torus is a fairly straightforward generalization of the flat circle we have already discussed. Those of us old enough to know the computer game Pac-Man know that the character and its ghost enemies are allowed to tunnel through the sides and top ends of the map to re-enter at the opposite side.

In the spirit of the quotient topology construction already discussed we can think of the top edge identified with the bottom edge and the left edge identified with the right. In order to depict this analogous to our circle construction we again draw the identifications together to first form a cylinder, and then by identifying the cylinder ends, we form a torus. Pac-Man's world looks flat to him, hence we call this torus the *flat torus*. Depicting Pac-Man's world on the more familiar circular torus shape again highlights how this depiction removed the discontinuity of the identification of his flat rectangular world. We can unroll or unwind the flat torus just as we did the circle.

This yields a tiling of the plane with identical copies of Pac-Man's



Figure 16: Pac-Man lives in a planar world with identifications between opposite tunnels (Image by Ajeet Gary).

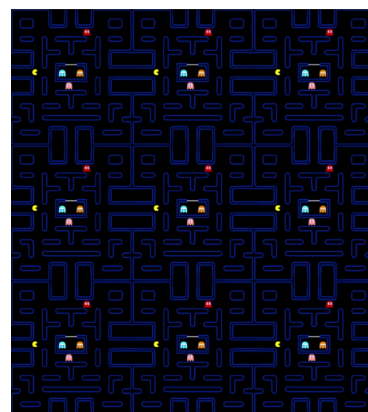


Figure 17: Cover of the torus. (Image by Ajeet Gary).

world. If we continue the tiling to infinity, we arrive at the universal cover of the torus (Figure 17). The unique space Pac-Man lives in is the *fundamental domain*  $[0, 1) \times [0, 1)$ .

The cover tiling is a repetition of this domain with integer differences "quotiented out" in both directions  $(\mathbb{R}/\mathbb{Z}) \times (\mathbb{R}/\mathbb{Z})$  and we can construct this plane by viewing the intervals as circles and rolling it along either direction  $S^1 \times S^1$ . Hence we get the torus as a product of the circle in each of the three views we discussed.

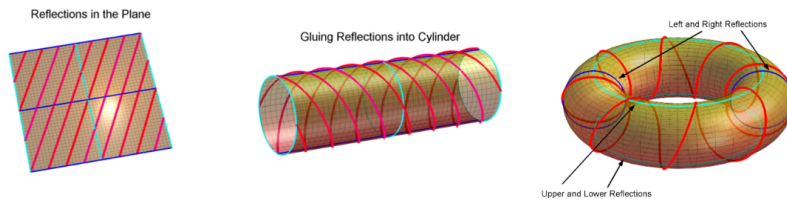
*The Image-Source method as an example of the Folded Torus*

Pac-Man serves as a familiar illustration of the flat torus structure but has no real reference to signal processing. An example much closer to signal processing is given by the well-known Image-Source method introduced by Allen and Berkeley<sup>3</sup>. The following Figure 18 is a reproduction of their original paper with some structure in it highlighted.

Surrounded by the red dashed line, we see that the pattern formed by the original "x" markings is periodically repeated in the plane, forming a planar rectangular tiling in the plane marked by the solid red lines. In our new language, we observe that the marked dashed rectangle is the fundamental domain of a flat torus, and that the plane tiling is the universal cover of this torus. While one can pick the original room with the circular listener in it as each of the four sub-segments of the fundamental domain, the fundamental domain has the same substructure of extra reflections inside this domain. Allen and Berkeley observed that the image behind a reflective wall makes the traveling path between listener and reflected source straight, hence giving a simple computation of the impulses from distance in this patterned plane.

One can construct the torus that has this property by taking a rectangular piece of paper and folding the piece of paper twice. The first fold yields a flat cylinder, and the second fold forms the *Folded Torus*. As we see, the folded torus is a flat torus with an additional fold in each direction, hence we have the product of two folded circles.

Both the toroidal construction by identifications and the effect of straightening paths on the torus is shown in Figure 19. Observe that



$[0, 1) \times [0, 1)$  is  $(\mathbb{R}/\mathbb{Z}) \times (\mathbb{R}/\mathbb{Z})$  is  $S^1 \times S^1$ . The torus is the Cartesian product of the three pictures derived from the quotient topology construction of the circle.

<sup>3</sup> Jont Allen and David Berkeley. Image method for efficiently simulating small-room acoustics. *The Journal of the Acoustical Society of America*, 65(4): 943–950, 1979

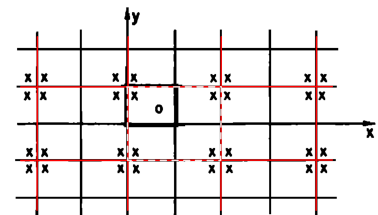


Figure 18: The torus topology underlying the Image-Source method of Allen and Berkeley. The dashed red line marks one of four possible fundamental domains, and the red tiling shows the tiling repetition of the universal cover.

The folded torus.

Figure 19: The torus construction maintaining fold information (Blue and Cyan). Red depicts a path under reflection.

reflections become linearized by unfolding the plane, but furthermore, they become windings first around the cylinder then around the torus. The winding number counts the number of times it winds around the circle in each direction. If these two numbers are integer and relative prime, they describe a closed circular path on the torus. If the quotient of these two numbers is not in the integers, but an irrational number, the path will eventually fill the whole torus. This state of affairs is known by a few names including *Kronecker fibration*. Integer windings describe various configurations of what are known as *Torus knots*.

This kind of construction is not exclusive to square domains. Circular and Elliptical domain shapes also reflect like a torus, a fact used by Keller and Rubinow <sup>4</sup> to model resonances on these shapes. The key ingredient is that they can be described by two independent coordinates and a coordinate preserving deformation from the square to the circle is shown in Figure 20 (redo figure).

### Combinatorial Construction of Topological Spaces

In many applications topological spaces naturally arise as one creates interconnectivity or combinations of entities. The case most familiar case for practitioners in signal processing are graphs, which then are made more specific as networks or dataflows, depending on the application. Graphs themselves just model connectivity. It is customary to define graphs by their collection of vertices and edges written as  $G = (V, E)$  with  $V = \{v_0, v_1, \dots, v_n\}$  and  $E = \{e_0, e_1, \dots, e_m\}$ . An interesting observation about this definition is that it treats edges and vertices as completely separate, though one usually thinks of edges as connecting vertices. The relationship of edges and vertices is introduced via some connectivity construction. Matrices can be used to capture this information. Two commonly used examples of matrices capturing connectivity information are the adjacency and the incidence matrices. Consider the following simple graph depicted in Figure 21.

The *adjacency matrix* captures a vertex to vertex relationship and has 1 as entry if an edge is present between a pair of vertices. Hence we can full out the adjacency matrix as follows:

$$A_G = \begin{matrix} & v_0 & v_1 & v_2 & v_3 \\ \begin{matrix} v_0 \\ v_1 \\ v_2 \\ v_3 \end{matrix} & \begin{pmatrix} 0 & 1 & 1 & 0 \\ 1 & 0 & 1 & 1 \\ 1 & 1 & 0 & 0 \\ 0 & 1 & 0 & 0 \end{pmatrix} \end{matrix}$$

The *incidence matrix* relates vertices to edges, and has a 1 entry if an

<sup>4</sup> Joseph Keller and Sol Rubinow. Asymptotic solution of eigenvalue problems. *Annals of Physics*, 9(1):24-75, 1960

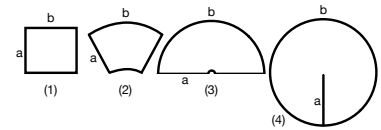


Figure 20: Deforming a square into a disk maintaining separate coordinates.

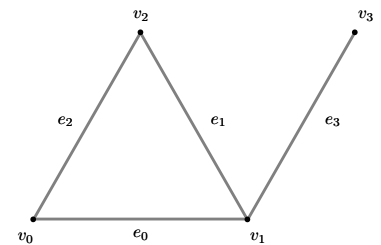


Figure 21: A simple Graph.



edge is "incident" to an edge (or vice versa!) and for the example graph we get the following matrix:

$$B_G = \begin{matrix} & e_0 & e_1 & e_2 & e_3 \\ \begin{matrix} v_0 \\ v_1 \\ v_2 \\ v_3 \end{matrix} & \begin{pmatrix} 1 & 0 & 1 & 0 \\ 1 & 1 & 0 & 1 \\ 0 & 1 & 1 & 0 \\ 0 & 0 & 0 & 1 \end{pmatrix} \end{matrix}$$

Matrix representation immediately invites a kind of algebraization of the graphs as we can now study properties of the matrix. This is in fact a way to enter into algebraic graph theory. In fact, the incidence matrix plays a much more important role in this algebraization. We will develop some of the reasons for this later.

*Simplicial Complex as Generalization of Graphs*

Simplices are higher-dimensional generalizations of vertices and lines. The next entity we need is something capturing the notion of area. The simplest possible combinatorial structure is that of an area captured by three points and surrounded by three edges (see Figure 22). This process can be continued. A volume can be

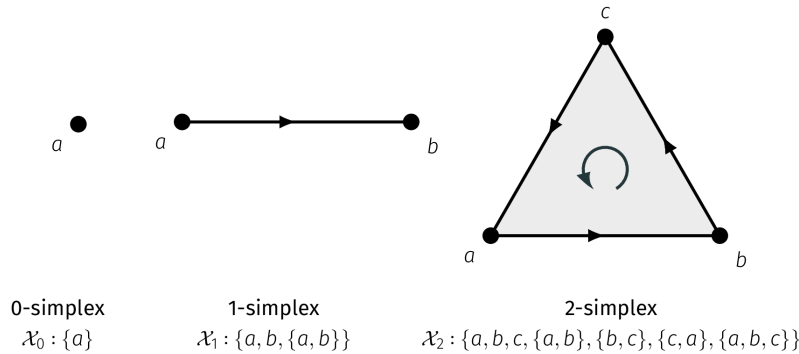


Figure 22: Low-dimensional simplices.

constructed by surrounding it by four triangles and so forth into higher dimensions. This can be described by sets just as we did for graphs, though we will organize our sets slightly differently. This justifies giving things a new name. A vertex will be called a 0-simplex and its set is simply a label for each vertex  $\mathcal{X}_0 = \{a\}$ . For all higher-order simplices we require that they include the sub-simplices from which it is built. In this setup, an edge also contains the vertices it connects and is now called a 1-simplex and its set description hence is  $\mathcal{X}_1 = \{a, b, \{a, b\}\}$ . This is just a somewhat different version of collecting vertex and edge information compared to our graph sets. However, we are now ready to write down the 2-simplex

$\mathcal{X}_2 = \{a, b, c, \{a, b\}, \{b, c\}, \{c, a\}, \{a, b, c\}\}$ . Observe that all the lower-order simplices in this set are just subsets of the largest one. This leads to data compression, because we can always construct the lower order simplices by set deletions. Set deletion also gives us a way to get sub-simplices as depicted in Figure 23. We can get a map to a face of an  $n$ -simplex by deleting one entry from its set, and it will return the  $n - 1$ -simplex opposite to the one we deleted. (Co)face maps is all we need to navigate a single simplex.

This map is hence named face-map and it takes us from an  $n$ -simplex to one of its  $n - 1$ -simplex faces. Sometimes, it is convenient to go in the other direction and the map is then called coface-map (the co-prefix refers to inverting the direction a map is taken).

An abstract simplicial complex consists of simplices that are connected together by the rule that they can only connect along shared (sub)simplices as seen in Figure 24. The word abstract here denotes that we do not think of a particular geometric configuration of the simplices in some space, so the notion of a simplex touching or penetrating another is not well defined. This should be familiar from graph theory as used for data-flow. Strictly we are only using that two points in a flow are connected, and some graphical depiction of the connection (whether it is for example a straight, or squiggly line or arrow) is an arbitrary choice to make this connection more visual or geometric.

### Computational Techniques

Next we will discuss two specific computational techniques from the realm of computational topology. These are selected from a wider range of algorithms for their breath of applicability to signal processing and sound synthesis.

#### (Persistent) Homology

Persistent homology is perhaps the mash hit of computational topological methods. At its heart is homology, which itself is extremely useful. In fact understanding homology is the key, and it has its uses outside of persistence. Hence we will start off discussing homology first.

#### Homology

Homology counts  $n$ -dimensional voids as well as the number of connected components of a topological space. For us (and in computational settings) these topological spaces will be simplicial complexes. To understand what we mean by an  $n$ -dimensional void consider

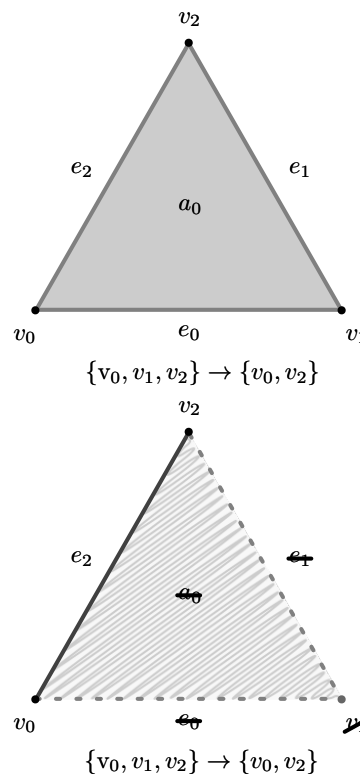


Figure 23: Deleting an entry in the set is the same as returning the face opposite the removed 0-simplex.

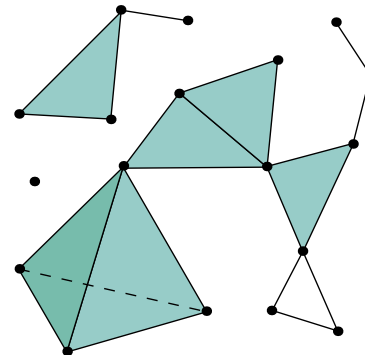
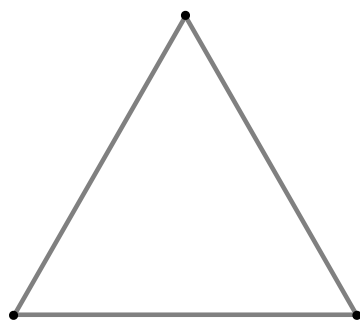
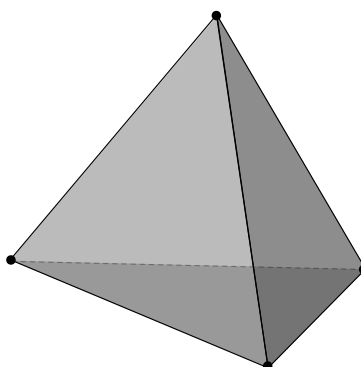


Figure 24: A simplicial complex.

the example depicted in Figure 25 showing two low-dimensional examples. A triangle bounds an empty area inside if it is not filled.



One "area-like" void



One "volume-like" void

Figure 25: A triangle can either be filled or empty inside. If it is empty inside we call this a *void*. The inside of an empty tetrahedron is also a void but of different dimensions. The first is "area-like" the second "volume-like".

This is an example of an "area-like" void, thinking of the dimensionality of the simplex that would fill it. It takes three lines to fence in this void, and we observe that in fact one only gets a  $n$ -void if it is fully bounded by such an  $n - 1$  fence. We see that this also holds for the example of the tetrahedron shape (from the boundary of a 3-simplex). The four 2-simplices that bound it enclose an "volume-like" void inside (if it is not filled in). It turns out that the algorithmic computations of these dimensional voids for simplicial complexes is fairly easy. Ultimately it turns out that we compute the rank information of two matrices, called boundary matrices to compute the number of voids. Stated like this, this may appear mysterious, but we have already noted that we only get a void when it is fully fenced in or bounded. But there is a second criterion: the fenced in area needs to indeed be empty and not be filled with an  $n$ -simplex. The aim here is to construct an algebraic setup in which we capture closed boundaries, which we will call *cycles* and denote by the letter  $Z$  (likely from the German "Zyklus"). Let's see how we get a cycle from the construction of a *boundary matrix*. Here we construct the boundary matrix from 1 - *simplices* to 0 - *simplices*. Recall that each 1-simplex in isolation is bounded by two 0-simplices. The boundary matrix captures this information for all 1-simplices in the simplicial complex. For simplicity we will consider here only a single 2-simplex and its boundary matrix  $\partial_1$  in Figure 26.

To populate our boundary matrix, we simply put a 1 for each vertex  $v_n$  that bounds a given edge  $e_m$ . We see that edge  $e_0$  is bounded by vertices  $v_0$  and  $v_1$  and hence we get the following column entries (Figure 27). We continue this process for all edges and arrive at a fully filled boundary matrix as depicted in Figure 28. While we simply entered 1 entries here, we can make all my arguments

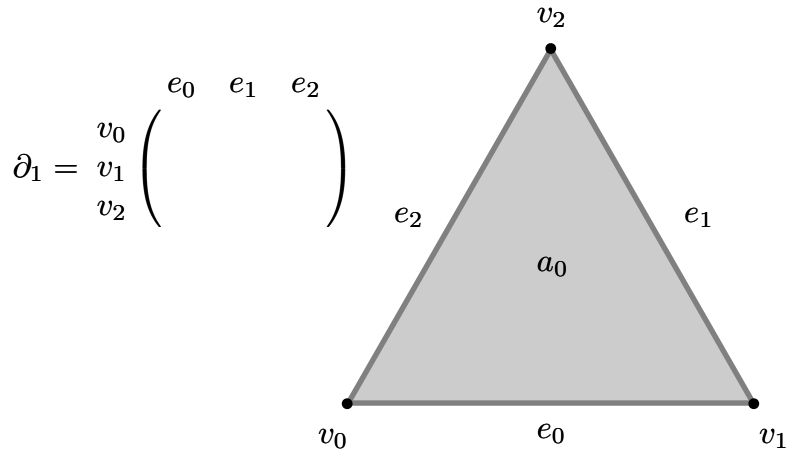


Figure 26: The boundary matrix of 1-simplices in a simple simplicial complex relates edges to bounding vertices.

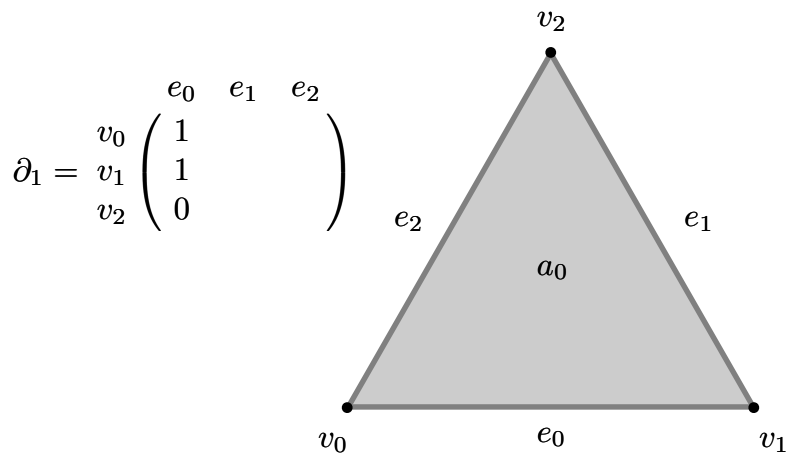


Figure 27: Two vertices  $v_0$  and  $v_1$  are bounding the edge  $e_0$ .

in this simple binary setting without overflow. This means that all our additions and subtractions are carried out by xor operations. To mathematicians, this is known as the cyclic finite group  $\mathbb{Z}/\mathbb{Z}_2$  and we can do linear algebra in this setting. Given that we can do linear algebra, we can add and subtract columns (or rows). Let us add the first two columns (Figure 29). Observe that the resulting vector is actually identical to the remaining edge column  $e_2$ ! That is these three columns are not linearly independent. Any pair of them is, but adding in the final column is not. We will not show a figure of this but you can easily check that the same holds for any chain of edges that eventually close on themselves in a cycle. In other words, if we sum over a closed chain of edges we get a zero vector and in our example we have  $\partial_1(e_0 + e_1 + e_2) = (0, 0, 0)^T$ . From linear algebra we know that linear dependence reduces rank. For every independent cycle (in the sense of linear algebra) we hence get a rank reduction. The size of the rank reduction is the size of the null-space of a linear

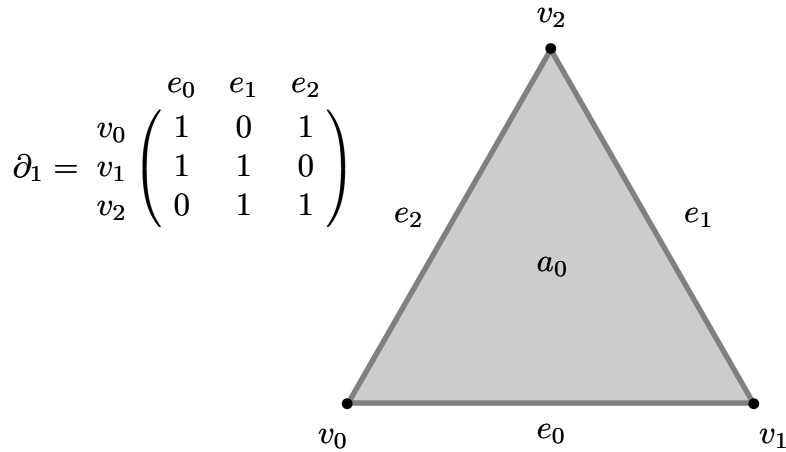


Figure 28: The completed boundary matrix from edges to vertices.

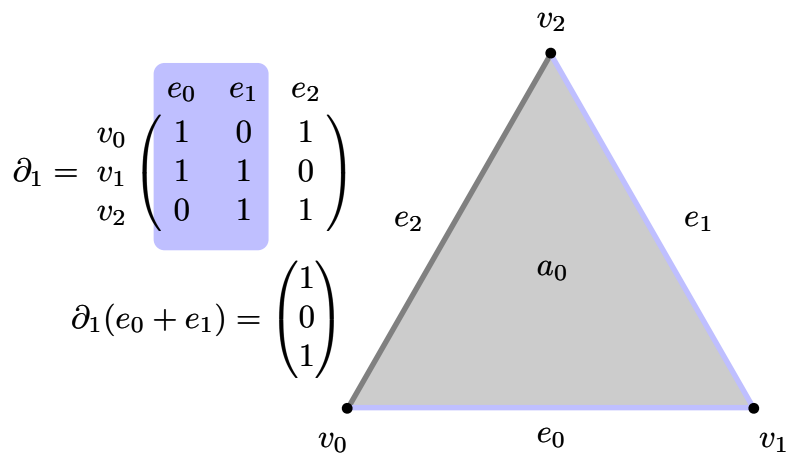


Figure 29: The linear combination of the first two columns.

map (here our matrix). This is the first key observation to computing homology.

Before we move on, let us consider a quick digression. We do this example in binary xor arithmetic. However the argument works for other coefficients as well. This allows us to capture more information. For example if we repeat the construction of the boundary matrix, but using a  $-1$  for the tip of a directed simplex arrow, and  $1$  for the base of such an arrow, we get the boundary matrix  $\partial_1$  shown in Figure 30. It is easy to check that again the sum of the three column equals the zero vector. We will however stick to the simple xor example for the rest of our discussion.

We are however not done computing homology just by computing the number of cycles. After all the very example we have showed a filling area  $a_0$ , hence the the cycle is actually filled hence does not bound a void. This is precisely the condition we are missing. We need to be able to differentiate if a cycle is filled in or not. The con-

Independent cycles lead to rank reduction in the boundary matrix.

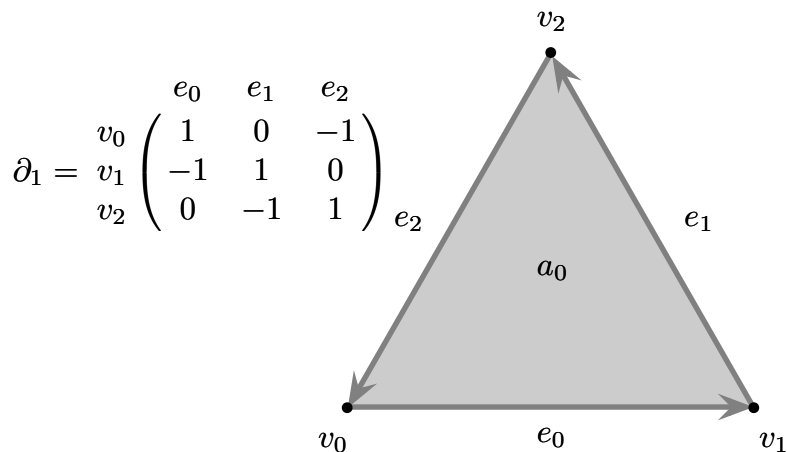


Figure 30: Boundary matrix of oriented 1-simplices. The addition of all three columns again leads to a zero vector.

dition is straightforward. Recall that each  $n$ -simplex by definition contains cycles that bound it. This information is encoded in the next higher-dimensional boundary matrix. So let us construct the  $\partial_2$  boundary matrix for both possible cases. A cycle of three edges is either bounding a void or is the boundary of an area (or in the simplicial language a 2-simplex). Both cases are shown in Figure 31.

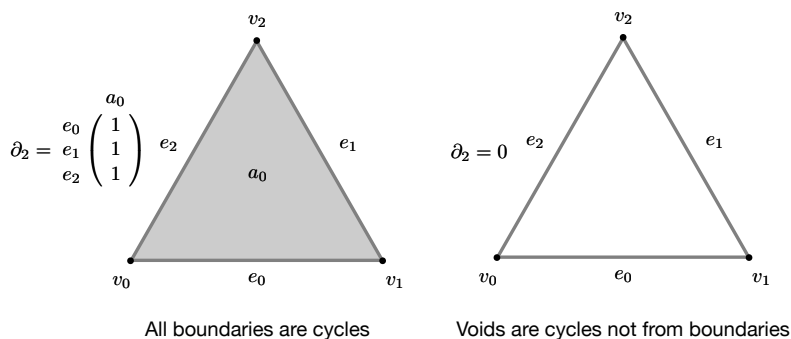


Figure 31: The boundary matrix  $\partial_2$  is capturing if a cycle is a void or the boundary of a filling simplex?

If the area is filled then the boundary map contains a map from the area to the three edges in its boundary. Given that we only have one area in this example we get only one column in the boundary matrix  $\partial_2$ . If, however, the cycle does not come from the boundary of an area there is no matching map in the boundary map. In other words cycles generated from being a boundary require a linearly independent entry in the boundary matrix, hence the rank must be containing all of them. Now we have all the pieces to compute homology. The information if something is in the cycle is in the lower dimensional boundary matrix, specifically the size of its null space. The information if something is filled in or not is contained in the higher dimensional boundary matrix, specifically the rank of the boundary matrix. All this is collected in this final Figure 32 on the

computation of the simplicial homology. It turns out that these re-

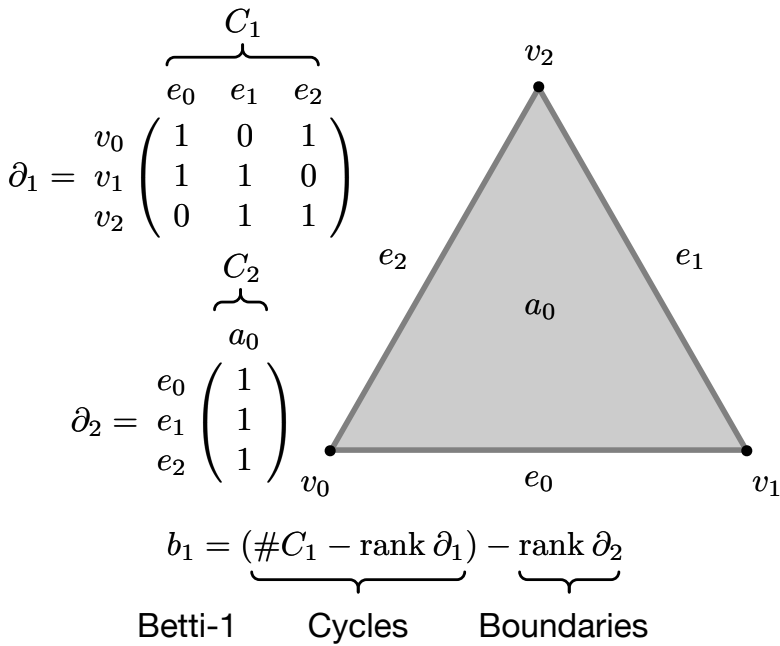


Figure 32: Computation of Betti-1  $b_1$ , the number of area-like voids.

relationships hold for any dimensional simplicial complexes and their boundary matrices derived analogous to how we did it for 1- and 2-simplices. So we get the formula for Betti numbers as shown in Figure 33. This, in a nutshell is the computation of homology of a

$$b_n = \underbrace{(\#C_n - \text{rank } \partial_n)}_{\text{Betti-n Cycles}} - \underbrace{\text{rank } \partial_{n+1}}_{\text{Boundaries}}$$

Figure 33: Computation of Betti-N  $b_n$ , the number of n-simplex-like voids.

simplicial complex! It amounts to computing the rank (and by simple extension the size of the null-space) of two matrices. There are a plethora of ways to compute the rank of a matrix, and variations of Gaussian elimination should come to mind. A particular form of a matrix, the *Smith Normal Form* can be computed by a Gaussian elimination style reduction and it makes reading off rank easy. A point to keep in mind here is that the specifics of the columns of the matrix does not matter for these results, merely that they are linearly (in)dependent as we discussed before.

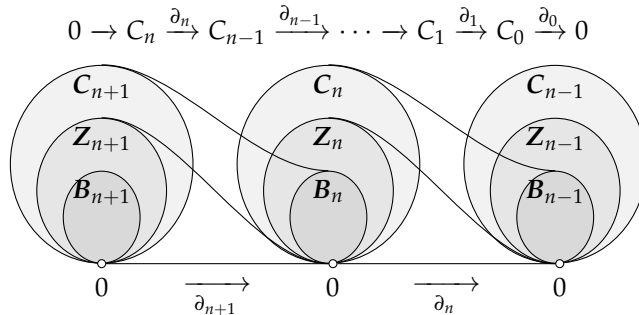
### Homology Groups

What we have discussed so far is how one computes homology for a simplicial complex. However, virtually all modern textbooks on



algebraic topology will describe homology through groups. To appreciate the connection of our discussion above in terms of constructed boundary matrices and rank-nullity computations here is a brief peek at the algebraic formulation of the same ideas.

The notion of an  $n$ -Chain  $C_n$  captures our process of constructing boundary matrices and what they operate upon. Chains that are connected via a sequence of boundary operators are called a *Chain complex*. As we have seen, some subset of chains can form cycles,



$$H_n = Z_n / B_n = \ker \partial_n / \text{im } \partial_{n+1}$$

which here is captured by  $Z_n$ . Furthermore, some chains are present because they are in the boundary of some higher dimensional element in a  $C_{n+1}$  chain, and therefore are in the *image* (or *im*) of the boundary map from  $\partial_{n+1} : C_{n+1} \rightarrow C_n$ . Furthermore recall that we noted that cycles  $Z_n$  are characterized by falling into the null-space which is also known as the kernel (or *ker*) of the boundary map  $\partial_n$ . Homology are the voids that are not from boundaries, hence we get the formula for the  $n$ th Homology group that is the cycles in the chain  $Z_n$  with the boundaries  $B_n$  in the chain "modded out" (that is removed), and we see that we can compute this information from the kernel and image of two boundary maps as we saw before.

Finally observe that the boundary of a boundary must always be zero, given that any boundary chains  $B_n$  are fully included in the cycles  $Z_n$  and all cycles are sent to 0 by the second boundary map. This fact is called the *fundamental lemma of Homology*.

$$\partial_n \partial_{n+1} = 0$$

Figure 34: Homology in the language of abelian groups and  $n$ -chains. The sequence of chains is called a chain complex.

Figure 35: The fundamental lemma of Homology states that a boundary does itself have no boundary.

To get a sense what homology looks like in concrete cases, here are some simple examples: Figure 36 shows a solid tetrahedron (that you can also think as an abstract 3-simplex) and next to it the boundary of said shape with the interior empty. We see that both cases are a single connected component ( $b_0 = 1$ ), while only the hollow shape has  $b_2 = 0$ . While computationally we will generally deal with simplicial complexes, remember that conceptually we are dealing with deformability, and if we inflate our hollow tetrahedron in the physical world we will arrive at something that looks like the surface of a sphere as seen in Figure 37. Next to it we depict the torus and its Betti numbers. The torus is characterized by two loops that cannot be collapsed as we have seen before and this is captured here by  $b_1 = 2$ .

Sometimes homological information is not presented in terms of Betti numbers but rather in terms of the structure of the Homology group. In our case, the groups are finitely generated. The cycles (without boundaries) are the generators in this group. Hence we can draw upon the structure theorem for finitely-generated abelian groups with respect to direct sums which is as follows:

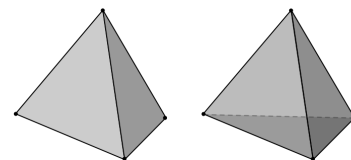
**Theorem.** A finitely-generated abelian group  $A$  can be uniquely expressed in the form of direct sums of finite numbers of free cyclic groups  $\mathbb{Z}$ , and cyclic groups  $\mathbb{Z}_{t_i}$  of finite period  $t_i$  called **Torsion**. The rank of the free group we will call **Betti numbers**, The indices  $t_i$  are not necessarily distinct prime and are called **torsion coefficients**:

$$A = \bigoplus_b \mathbb{Z} \oplus \bigoplus_i \mathbb{Z}_{t_i}$$

In this view, Betti numbers count the number of free groups  $\mathbb{Z}$  and hence the homology groups for the sphere and torus written as shown in Figure 38. In our discussion we have ignored the *Torsion* coefficients that show up in this structure theorem. If we use our xor linear algebra, torsion never occurs, but it can occur if we consider oriented situations. However, so far torsion coefficients have not made a particular impression in applied topological examples, so we will continue to ignore them in this introduction. But it is good to know they exist!

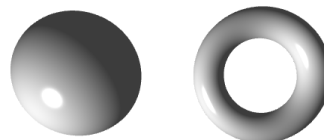
### Persistent Homology

The idea of persistence is fairly straightforward. We can compute homology for any simplicial complex, so of course we can compute homology for a sequence of additions to a simplicial complex. The



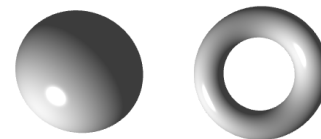
$b_0$	1	1
$b_1$	0	0
$b_2$	0	1

Figure 36: The Betti numbers of the simplicial ball and sphere.



$b_0$	1	1
$b_1$	0	2
$b_2$	1	1

Figure 37: The Betti numbers of the ball and torus.



$H_0$	$\mathbb{Z}$	$\mathbb{Z}$
$H_1$	0	$\mathbb{Z} \oplus \mathbb{Z}$
$H_2$	$\mathbb{Z}$	$\mathbb{Z}$

Figure 38: The homology groups of the ball and torus.

Betti numbers will change as simplices are included, such as cycles are formed by closing the loop, or cycles become boundaries by filling simplices being added.

If we consider a complete simplicial complex  $X$  but imagine that its piece were successively added (but nothing ever removed) we get a sequence of simplicial complexes  $X_m$  starting with some starting simplex  $X_0$ . This sequence of inserting of simplices lead to a finite *filtration*:

$$0 \hookrightarrow X_0 \hookrightarrow X_1 \hookrightarrow \dots \hookrightarrow X_{m-1} \hookrightarrow X_m = X$$

Given that each  $X_m$  is a simplicial complex on its own we can of course compute its homology with the algorithm we have seen. For example, we can compute the  $n$ -homology after each insertion. This will capture how the homology changes as we keep inserting simplices.

$$\begin{array}{ccccccc} X_0 & \hookrightarrow & X_1 & \hookrightarrow & \dots & \hookrightarrow & X_m \\ \downarrow H_n & & \downarrow H_n & & \dots & & \downarrow H_n \\ H_n(X_0) & & H_n(X_1) & & \dots & & H_n(X_m) \end{array}$$

This process of course works for any sequence of inserting simplices, but persistence is usually introduced through some metric process that dictate how simplices are inserted. To get an intuition of this, consider starting out just with 0-simplicies, that is a cloud of points. The process we are considering here is named after *Vietoris-Rips*. The rule is that if you grow a spherical neighborhoo, and two neighborhoo's touch, you add an edge. If three neighborhoo's touch you add a 2-simplex, for 4 a 3-simplex, and so fourth. This process is depicted for an example of a sampled circle with noise in Figure 39. Imagine you do not know where the sampled point is from and you want to recover a possible topology that explains it. If it is from a circle, we should hopefully recover the circle topology.

The output of process can be represented visually as *barcodes*. They capture when a homological feature emerges and is destroyed. Features emerge as cycles form, and they are destroyed as cycles are filled in hence become cycles from boundaries. So, a barcode captures the birth and death of homology and persistence has its name by the intuition that salient topological features will *persist* longer than features that emerge from noisy process or are more fine grain or local. We see that when the big cycle first forms, there are a few more smaller cycles that also form due to the distribution of the random samples, but those smaller cycles fill in faster and hence disappear faster than the big cycle.

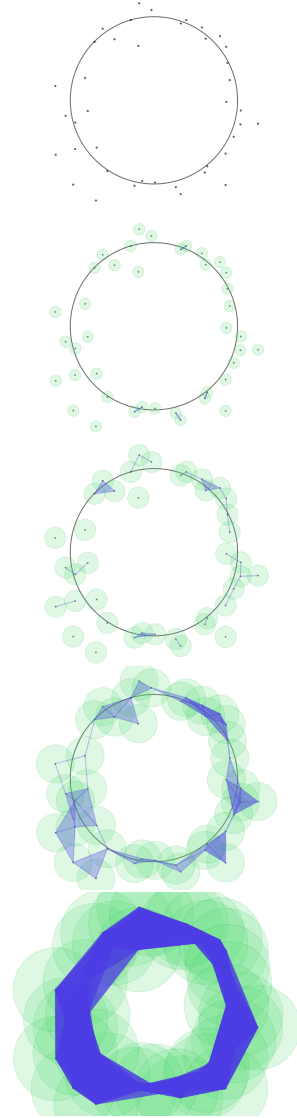


Figure 39: The Vietoris-Rips process. As growing radii touch, simplices are connected and become higher order. Notice that the *persistent* feature is the hole of the circle.

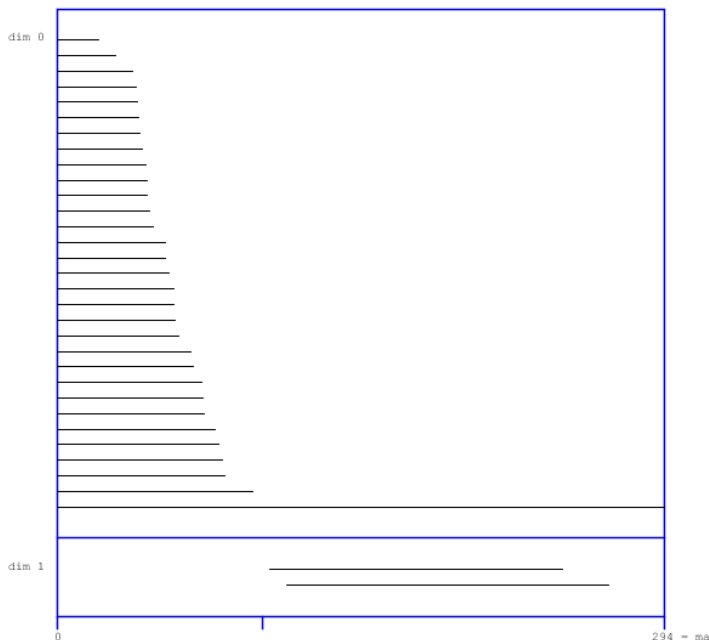


Figure 40 shows a practical example of a bar code output from one of the many implementations that exist. This picture is captured from JavaPlex with the visual interface realised in Processing. The dataset here is a handdrawn pattern of a point cloud roughly capturing a figure-8 style arrangement. The 0-homology captures the change in connected components, which shrinks as more and more points become connected. The 1-homology indeed picks up two loops as one would hope. The blue marker at the bottom of the barcode shows the Vietoris-Rips radius used for the snapshot simplicial complex on the right. We see that at that instance the cycles have not quite closed yet.

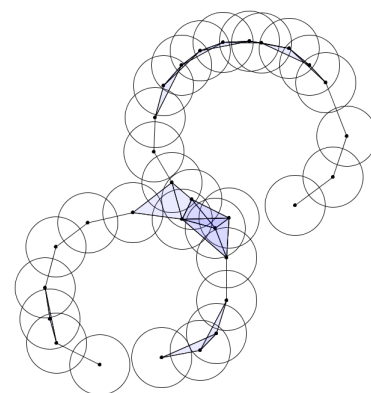


Figure 40: Barcodes for the 0- and 1-homology of a figure-8 style point cloud.

### Embedding and Time-Series

So far we have talked about point clouds, but audio is typically a sequence of samples without any particularly interesting geometric configuration. One way to make time series more geometrical and extract features from them is embedding the samples in a higher-dimensional space. Another view that can be relevant relates to simplicial complexes that we defined combinatorially, and how to make them into geometric objects. So there is a question of how to place a topological information into a space. Figure 41 shows a range of examples of how a topological circle can be placed into the plane. The leftmost group consists of curves that do not self-intersect. These are called *embeddings*. If there are isolated self-intersections it is called an *immersion*. However, a general continuous map does not need to

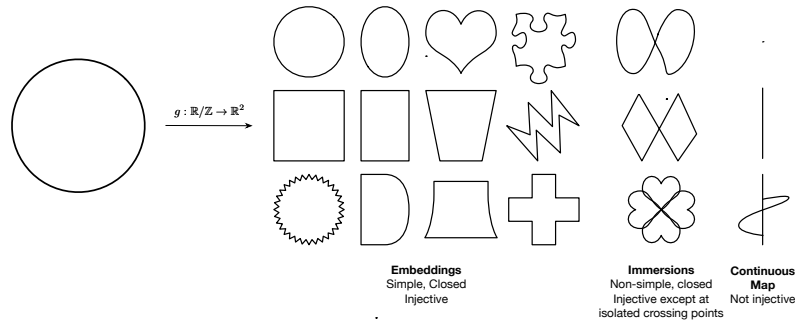


Figure 41: A topological circle can sit in the plane (left) without intersections (embedding), (middle) local intersections (immersion) and (right) lots of overlap (from a continuous map).

be an immersion or embedding. Some examples of this are seen on the right in Figure 41. Given that they are continuous maps from the circle, they have an underlying continuous parametrization in the topology of a circle.

A particularly popular approach to embed a time-series is known as either time-delay or *Takens embedding*. The latter name comes from the work by Florens Takens who has proved that embeddings using these time delay constructions do exist as long as one embeds into a high enough dimensional space, and with some *genericity* assumptions. We will not cover the details here but will work on some intuitions.

Given a time function, one can sample the time functions at different delays. A *time-delay embedding* creates coordinates at fixed delayed intervals  $t_d$  from a given point in time  $t$ . Hence we get coordinates  $(x_0(t), x_1(t + t_d), \dots, x_n(t + nt_d))$  for an  $n$ -dimensional embedding. We can view this as a short-term discrete window with a set unit delay of  $t_d$ . Figure 42 shows the time-delay embedding of a sinusoid into the plane. We should expect a time delay of  $\frac{\pi}{2}$  to give us the circle. Other time delays give us circle topologies but they embed as skewed ovals of some sort. There is, however, a *degenerate* case, when the delay is an integer multiple of  $\pi$  as depicted in the bottom case. Then we do not get an embedding but a line with multiplicity 2 everywhere except at the extremes. Even adding higher dimensions, that is more delay coordinates at the same delay will never not keep this a line. This is perhaps the simplest example of why the embedding result of Takens needs genericity assumptions. Things are still good though, because even a tiny deviation will give us an embedding, and in general we expect that almost all time delays will give us an embedding.

Consider the next example, which is a somewhat more complicated waveform (Figure 43). The top embedding self-intersects, and even wiggling a little bit will not resolve this self-intersection, but will merely move it around somewhat. If we allow ourselves larger

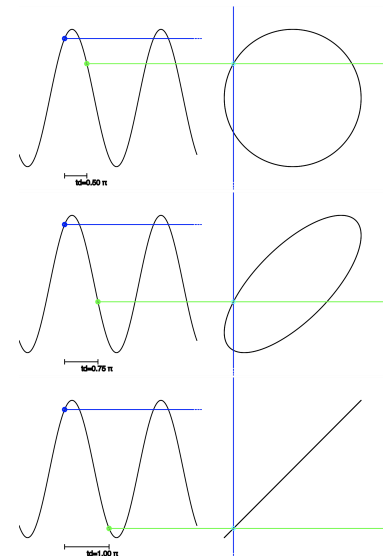


Figure 42: Embeddings of a sinusoid into the plane with one time delay with different delays. For multiples of  $\pi$  this does not actually give an embedding, both otherwise it does.

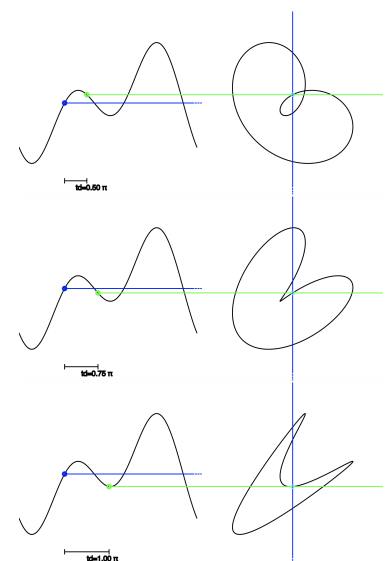
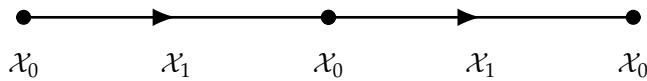


Figure 43: Embeddings of a non-sinusoidal function into the plane with one time delay with different delays.

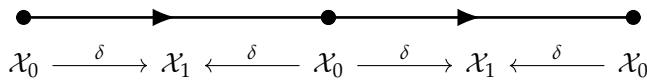
changes in time-delay we can however find delays at which it is an embedding, but it is not generically true for this function. However if you look at the lower two figures as side-projections of a 3-dimensional embedding it suggests that indeed lifting this curve into another dimension will resolve the crossing hence, generically, lead to embeddings. This is precisely what happens and the intuitions how crossings of complicated functions can be resolved by giving more dimensional space.

*Topological Filters via Sheaves*

Sheaves provide a way to attach data to a topological space. The mechanism is very general because what we mean here by data is very general. Sheaf theory is much more general than we will discuss here. Our sheaves are attached over simplicial complexes. Consider a simple example of a *line complex* which is the repeated alternation of a 0-simplex and a 1-simplex mirroring the pattern of a connected sampled line.

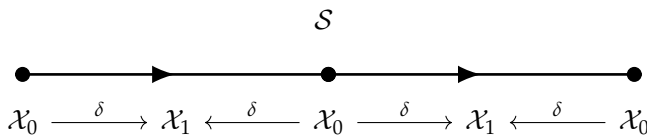


We can relate simplices via (co)face maps. In this example we pick the coface map  $\delta$ .

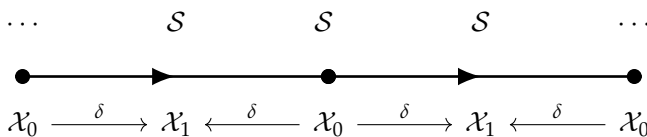


Navigations between simplices in a line complex via coface maps.

We will denote some data attached to a simplex by  $\mathcal{S}$ .



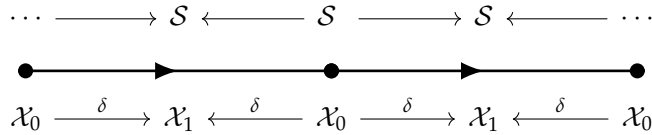
The definition of a sheaf requires that we attach data  $\mathcal{S}$  to each simplex  $\mathcal{X}_\bullet$ .



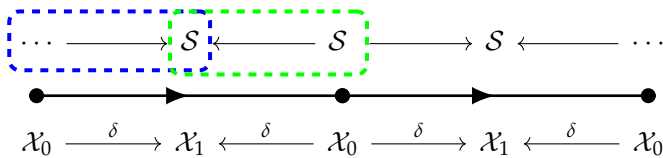
Sheaves consist of data  $\mathcal{S}$  attached to each simplex.

A sheaf construction further requires that whenever there is a map between simplices, we have to provide a map between the attached data.

Sheaves also require that for each map between simplices we provide a map between sheaf data.



Notice that typically we have more than one map pointing to the same data  $\mathcal{S}$ . This leads to a final requirement for sheaves. Informally we have to avoid that there is a conflict between these two maps. They have to in some suitable sense agree what  $\mathcal{S}$  is. This can be thought of in two ways. The first is via composition. One can require that the two maps can be *composed*. Another way to think about this is to require that local data has to be *consistent*. With these three rules we have a full definition of a sheaf over a simplicial complex. In examples we will see how that is realized in practice soon.

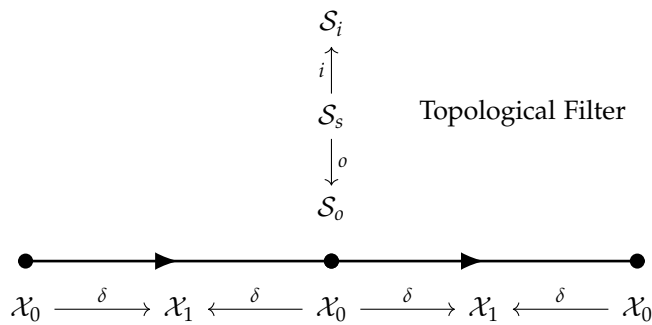


Sheaves maps are required to allow composition. Alternatively we can think of local sheaf data being required to be consistent.

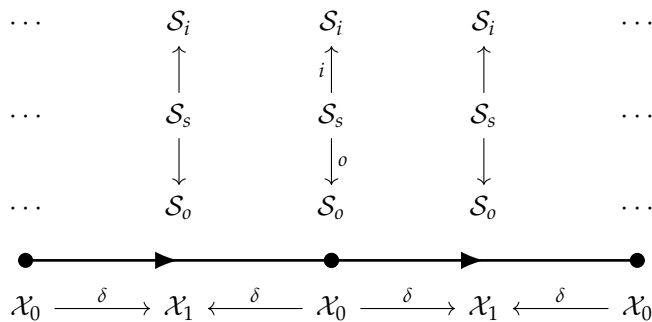
We are interested in one particular sheaf structure called *topological filters* as invented by Michael Robinson<sup>5</sup>. A topological filter assume the typical structure that we assume a filter to have. It separates input, state and output. Later we will see that this structure can be used both for classical linear time-invariant filters as well as non-linear oscillatory structures.

<sup>5</sup> Michael Robinson. *Topological signal processing*. Springer, 2014

A topological filter has input, state, and output data connected by computation.

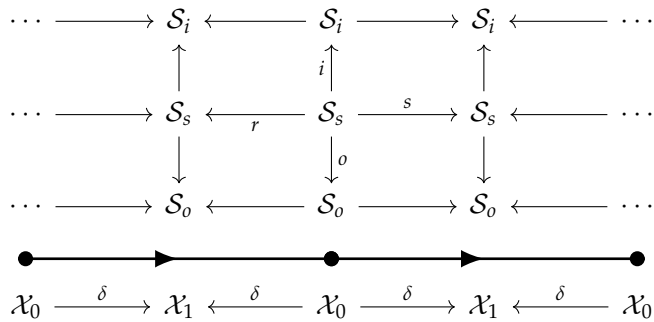


By the rules of sheaves we replicate this structure over all simplices.





And we have to provide maps between all the data.



To understand how to place general linear time-invariant filters into this sheaf formalism consider, the structure of the Direct-II form is particularly convenient (Figure 44) for the filter equation:

$$y = \sum_{i=1}^N b_i \cdot x_{N-i} + b_0 \cdot x + \sum_{j=1}^N -a_j \cdot y_{N-j}$$

This filter structure suggests that our sheaf state should capture the

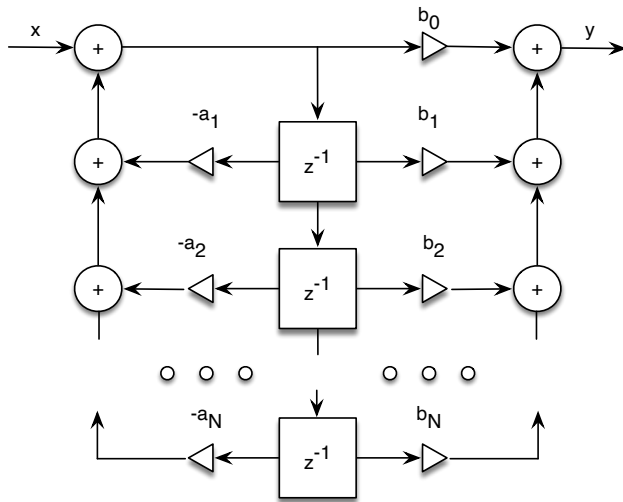
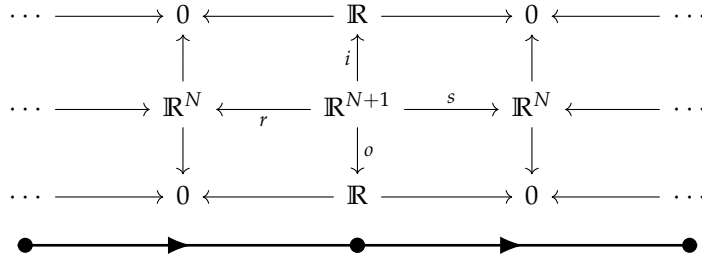


Figure 44: General LTI filter in Direct-II form.

shift register information. We can model this as a finite vector space  $\mathbb{R}^N$ . At a local position, we have a given input  $i$  that is injected into the state and leading to an augmented state  $\mathbb{R}^{N+1}$ . From this we can derive the output map  $o$  being the feedforward computation of the filter. The map  $s$  captures both the shift of the register and the feedback computation. Maps  $i$  and  $r$  simple inject information into the next step. Given that there is no input over 1-simplices the state over them is  $\mathbb{R}^N$ . Input and output in this construction are isolated audio samples in  $\mathbb{R}$ . Hence we get the following sheaf structure for general linear time invariant filter formulated as topological filters:

LTI filters maps for topological filters.



The following sheaf maps are equivalent to the filter equation:

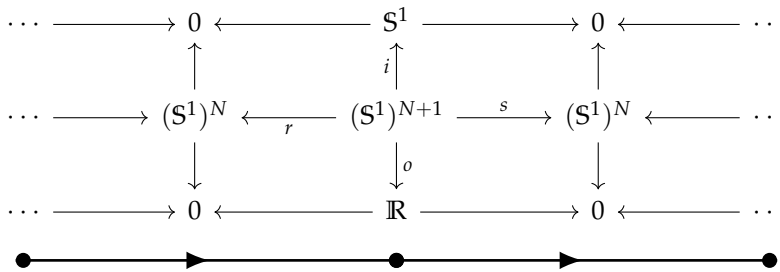
$$\begin{aligned}
 s &: (x_0, x_1, \dots, x_{N-1}, x) \rightarrow (x_1, x_2, \dots, x_{N-1}, \\
 &\quad x + \sum_{j=1}^N -a_j \cdot x_{N-j}) \\
 r &: (x_0, x_1, \dots, x_{N-1}, x) \rightarrow (x_0, x_1, \dots, x_{N-1}) \\
 i &: (x_0, x_1, \dots, x_{N-1}, x) \rightarrow (x) \\
 o &: (x_0, x_1, \dots, x_{N-1}, x) \rightarrow (b_0 \cdot x + \sum_{i=1}^N b_i \cdot x_{N-i})
 \end{aligned}$$

Maps  $i$  and  $r$  just copy information around, so we are left with maps  $s$  and  $o$  to do actual computation. The  $s$ -map captures the dynamical update of the filter, while the  $o$  captures the static feed-forward computation locally. The sheaf construction alone allows us to read of properties of digital filters. For example the feed-forward computation is unconditionally stable because it does no longer interact with any other data on the sheaf, as it is surrounded by 0-maps on the output side. With this construction any general IIR filter can be associated with a topological path construction.

But the construction is not confined to linear filters. Highly nonlinear computations can also be treated in this framework. If instead of vectors in a vector space we consider ensembles of circle and maps between them, we can capture many oscillatory sound synthesis methods and topologize them in essentially the same way. Consider this sheaf structure:

Sheaf maps can be nonlinear.

Topological filters using maps between ensemble of circles.



Perhaps one of the more prominent examples of oscillatory phenomena is *Frequency Modulation* (or just *FM*).

$$\begin{aligned}
 s : (x_0, z_0, x) &\rightarrow (x_0 + \Omega + H \sin(2\pi z_0) + x \pmod{1} \\
 &\quad, z_0 + \omega_m \pmod{1}) \\
 r : (x_0, z_0, x) &\rightarrow (x_0, z_0) \\
 i : (x_0, z_0, x) &\rightarrow (x) \\
 o : (x_0, z_0, x) &\rightarrow (\sin(2\pi x_0 + \phi))
 \end{aligned}$$

But whatever the computations are that are formalized in this way, we can now associate them with topological construction and perform the computations.

Figure 45 shows a line path that winds around a torus and closes onto itself. We can use this to create metric information that specifies the distance between sample points. Standard digital filter algorithms, such as simple resonators using BiQuad filters, or plugged string simulations using Karplus-Strong can be realized using the LTI-based sheaf filter, and FM and many other oscillatory methods can be realized using the circle map sheaf.

### *Epilogue — More to know that we did not cover*

The fields of topological signal processing and topological data analysis are much richer than could be covered here. For example topics such as *Graph Signal Processing*, *Combinatorial Hodge Theory*, *Sheaf Cohomology*, *Topological Features in Machine Learning* have all been left out completely. All of them are however interesting and worthwhile to learn about.

### *Vistas for future research*

Despite its substantial history topological data analysis and topological signal processing have left many open research avenues ripe for exploration. In particular in the real of audio signal processing there remains much to be done. Here are but two of many possible topics of interest: *Topological Harmonic Analysis - Build bridge between Persistence and Fourier*, *Sheaves over higher order topologies*.

### *Further Reading*

To learn more details and cover gaps in the material discussed here, the following are good yet fairly accessible long form treatments.

- Edelsbrunner & Harer, *Computational Topology*, 2010.

Sheaf maps for frequency modulation.

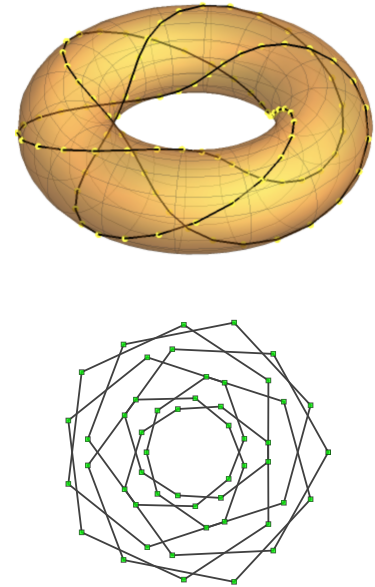


Figure 45: A close line complex on a torus and its top projection. It gives variation in distance that is used to render sound.

- Robinson, Topological Signal Processing, 2014.
- Ghrist, Elementary Applied Topology, 2014.
- Perea, Jose A. "Topological time series analysis." Notices of the AMS 66:5 (2019).

### *Software Recommendations*

The landscape of software implementation of topological algorithms is already fairly vast and rapidly expanding. This is a very small selection curated for either ease of use, relevance to signal processing, or performance.

- (Java)Plex (C++,Java) - Persistent Homology: Accessible with visual frontend (Processing/Java)
- Ripser (C++) - Persistent Homology: Fast
- Teaspoon (Python) - Assorted methods including Topological Signal Processing

### *Acknowledgements*

I owe Gianpaolo Evangelista, chair of DAFx-2022 my gratitude for offering the time to present this material during two tutorial sessions at the conference. These notes have benefitted from feedback of numerous tutorial attendees, in particular Lauri Savioja for extensive discussion and helpful suggestions for improvements. Figure 41 is from a 2022 DAFx paper by the author. Figures 16 and 17 are snapshots from very nice movie visualizations made by Ajeet Gary, used here and in the DAFx tutorial presentation with his kind permission. Last but not least the material presented is part of a larger book project with the generous support of a Simon Guggenheim Foundation fellowship. Figure 24 is a public domain figure from wikipedia.

### *References*

- Jont Allen and David Berkley. Image method for efficiently simulating small-room acoustics. *The Journal of the Acoustical Society of America*, 65(4):943–950, 1979.
- Georg Essl. Iterative phase functions on the circle and their projections: Connecting circle maps, waveshaping, and phase modulation. In Richard Kronland-Martinet, Sølvi Ystad, and Mitsuko Aramaki, editors, *Perception, Representations, Image, Sound, Music*, pages 681–698. Springer, 2021. ISBN 978-3-030-70210-6.

Joseph Keller and Sol Rubirow. Asymptotic solution of eigenvalue problems. *Annals of Physics*, 9(1):24–75, 1960.

Michael Robinson. *Topological signal processing*. Springer, 2014.

Ken Steiglitz. *A Digital Signal Processing Primer, with Applications to Digital Audio and Computer Music*. Addison Wesley, 1997.